SLAC–PUB–13756
August, 2009

Polarized Antenna Splitting Functions

Andrew J. Larkoski and Michael E. Peskin[1]

SLAC, Stanford University, Menlo Park, CA 94025 USA

ABSTRACT

We consider parton showers based on radiation from QCD dipoles or 'antennae'. These showers are built from $2 \to 3$ parton splitting processes. The question then arises of what functions replace the Altarelli-Parisi splitting functions in this approach. We give a detailed answer to this question, applicable to antenna showers in which partons carry definite helicity, and to both initial- and final-state emissions.

Submitted to *Physical Review* **D**

[1]Work supported by the US Department of Energy, contract DE–AC02–76SF00515.

Contents

1 Introduction **1**

2 Proposal for the $2 \to 3$ splitting functions **2**

3 Spin-0 case **6**

4 Spin-1 and spin-2 case **9**

5 Spin-$\frac{1}{2}$ and spin-$\frac{3}{2}$ cases **12**

6 Initial-state showers **14**

7 Comparison to previous results **19**

1 Introduction

In the studies that are now being done to prepare for physics at the LHC, many new approaches have been proposed to the old problem of generating parton showers. The workhorse event generators PYTHIA [1] and HERWIG [2] generate parton showers by successive radiations from individual partons. The 'splitting functions' that defines the radiation pattern are taken to be the kernels in the Altarelli-Parisi equation [3,4]. This guarantees that the radiation pattern is correct in the region in which two partons become collinear. Marchesini and Webber pointed out that it is also important to include color interference between emissions from different partons [5]. In the workhorse generators, this is implemented by angular ordering of emissions.

The program ARIADNE, by Andersson, Gustafson, Lönnblad, and Pettersson, took a different approach, implementing color coherence by considering the QCD dipole to be the basic object that radiates a parton [6,7]. The basic branching process in a parton shower is then a splitting in which two partons forming a color dipole radiate a third parton. This approach has been taken up recently by a number of authors. It is the basis for the VINCIA shower by Giele, Kosower, and Skands [8] and the parton shower implementation in SHERPA by Krauss and Winter [9]. We are also developing a parton shower based on this approach [10]. In the years between ARIADNE and the newer works, the term 'dipole' has been applied in QCD to a different strategy based on $1 \to 2$ splittings with recoil taken up by a third particle [11]. To avoid confusion, we will follow [8] in calling the initial two-parton state an 'antenna' and a branching process with $2 \to 3$ splittings an 'antenna shower'.

Central to the antenna shower is the $2 \to 3$ splitting function, the function that gives the relative branching probabilities as a function of the final momenta. The original ARIADNE program used an *ad hoc* proposal satisfying the basic consistency requirements. It would be better to have a prescription that can be directly derived from QCD. Splitting to three partons has been studied in great detail in the QCD literature, but not for this application. Collinear systems of three partons are a part of the infrared structure of QCD at next-to-next-to-leading order. and calculations that reach this level need an explicit prescription for treating this set of infrared singularities. Kosower [12] defined the 'antenna function' as a basic starting point for the analysis of this problem. Many authors have computed antenna functions [13–15]. Quite recently, Gehrmann-De Ridder, Gehrmann, and Glover have built a complete formalism of 'antenna subtraction' for NNLO calculations [16]. The kernel in their theory can be interpreted as a $2 \to 3$ splitting function, and it has been used to perform $2 \to 3$ splitting in the VINCIA shower [8].

In this paper, we will take a much more direct route to the construction of $2 \to 3$ splitting functions. We will compute these functions by writing local operators that

create two-parton final states and computing their 3-parton matrix elements. These calculations are very straightforward. They can be used to treat individually all possible sets of polarized initial and final partons.

This paper is organized as follows: In Section 2, we will present our complete set of polarized $2 \to 3$ splitting functions. In Section 3, we will give the derivation for the cases with total spin zero. In Sections 4 and 5, we will give the derivation for the cases with nonzero total spin.

All of these derivations will be done in the kinematics of final-state radiation. This is the easiest situation to visualize and understand. However, the same splitting functions can be used, after crossing, to describe parton emissions that involve initial-state particles. We will explain how to use our expressions for initial-state showers in Section 6.

The $1 \to 2$ Altarelli-Parisi splitting functions are universal in the sense that they result from a well-defined singular limit of QCD amplitudes. For $2 \to 3$ splitting functions there is no such universality. The collinear and soft limits must agree with the known universal values, but away from these limits there is no unique prescription. Earlier in this introduction, we made reference to a number of previous proposals for the spin-averaged antenna splitting functions. All of these, including the ARIADNE splitting functions, have the correct soft and collinear limits and so satisfy the basic requirements. In Section 7, we will give a detailed comparison of the $2 \to 3$ splitting functions obtained using our method to previous proposals for these splitting functions.

2 Proposal for the $2 \to 3$ splitting functions

We begin by defining variables for $2 \to 3$ splitting. There are three cases of splittings that are needed for antenna showers: the final-final (FF) splitting, in which a third particle is created by coherent radiation from a two-particle system in the final state; the initial-final (IF) splitting, in which a third particle is created by coherent radiation from an initial- and a final-state particle; and initial-initial (II) splitting, in which a third particle is created by coherent radiation from two initial-state particles. It is easiest to understand the kinematics of antenna splitting for the FF case. In this section, we will explain this kinematics and give a precise prescription for the splitting functions. In Section 6, we will extend our prescription to the IF and II cases, in such a way that the same splitting functions can be used in those cases.

Consider, then, a two-parton final-state system (A, B) that splits to a 3-parton system (a, c, b), conserving momentum, as shown in Fig. 1(a). Let $s_{ij} = (k_i + k_j)^2$,

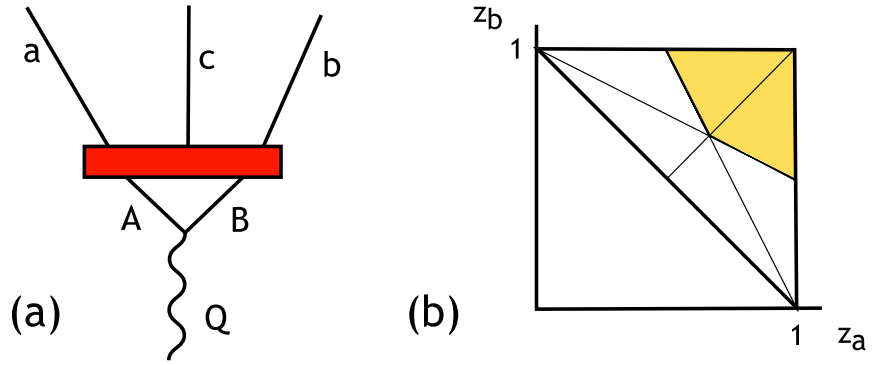

Figure 1: (a) Kinematics of $2 \to 3$ splitting in the final state (FF) case. (b) Phase space for $2 \to 3$ splitting in the FF case. The six regions corresponding to different orderings of s_{ab}, s_{ac}, s_{bc} are shown. The region that should be well described by an antenna splitting $AB \to acb$ is shaded.

and let $Q = k_A + k_B = k_a + k_b + k_c$.

The fractional invariant masses in the final state are

$$y_{ab} = \frac{s_{ab}}{s_{AB}} \ , \quad y_{ac} = \frac{s_{ac}}{s_{AB}} \ , \quad y_{bc} = \frac{s_{bc}}{s_{AB}} \ . \tag{1}$$

The momentum fractions of the three particles in the (AB) frame are

$$z_a = \frac{2Q \cdot k_a}{s_{AB}} \ , \quad z_b = \frac{2Q \cdot k_b}{s_{AB}} \ , \quad z_c = \frac{2Q \cdot k_c}{s_{AB}} \ . \tag{2}$$

These obey the identities

$$y_{ab} = (1 - z_c) \ , \quad y_{ac} = (1 - z_b) \ , \quad y_{bc} = (1 - z_a) \ . \tag{3}$$

and

$$y_{ab} + y_{ac} + y_{bc} = 1 \ , \quad z_a + z_b + z_c = 2 \ . \tag{4}$$

The FF phase space covers the triangle $z_a \leq 1$, $z_b \leq 1$, $z_a + z_b \geq 1$. We can divide this phase space into six triangles, each of which has a different ordering of the three quantities y_{ab}, y_{ac}, y_{bc}, as shown in Fig. 1(b). An antenna shower should give an accurate description of the dynamics in the two regions $y_{ac} < y_{bc} < y_{ab}$, $y_{bc} < y_{ac} < y_{ab}$ that are shaded in the figure.

Radiation from different QCD antenna is strictly indepedent and non-interfering only in the limit of a large number of colors in QCD, $N_c \gg 1$. Keeping only terms

leading in N_c is known to be a good approximation to full QCD in many circumstances. In particular, parton shower algorithms are correct only to leading order in N_c. In this paper, we will explicitly work only to the leading order for large N_c.

In this context, the rate for a $2 \to 3$ splitting is given by a formula of the form

$$N_c \frac{\alpha_s}{4\pi} \int dz_a dz_b \ \cdot \mathcal{S}(z_a, z_b, z_c) \tag{5}$$

For example, in $e^+e^- \to q_- g_+ \overline{q}_+$,

$$\frac{1}{\sigma_0} \frac{d\sigma}{dz_a dz_b} = N_c \frac{\alpha_s}{4\pi} \frac{z_a^2}{(1-z_a)(1-z_b)} \ , \tag{6}$$

where (a, c, b) are the $(q, g, \overline{q})$, respectively, $-$ and $+$ denote left- and right-handed helicity, and σ_0 is the cross section for $e^+e^- \to q_- \overline{q}_+$ [17]. Eq. (5) will be our basic formula of reference. Using this notation, we can write the various $2 \to 3$ splitting functions as

$$\mathcal{S} = \frac{\mathcal{N}(z_a, z_b, z_c)}{y_{ab} y_{ac} y_{bc}} \ , \tag{7}$$

where the numerator is a simple function of the z_i. For example, for the splitting $q_- \overline{q}_+ \to q_- g_+ \overline{q}_+$ given above,

$$\mathcal{N} = y_{ab} z_a^2 = (1 - z_c) z_a^2 \ . \tag{8}$$

In Table 1, we give our proposal for the numerator functions for all possible cases of massless quark and gluon splittings. The expressions are all monomials in the y_{ij} and z_j.

In the FF kinematics, $\mathcal{S}(z_a, z_b, z_c)$ in (7) is always positive. In IF and II kinematics, as we will explain in Section 6, the situation is more subtle. First, the y_{ij} may be negative, leading to a negative value of (7). This happens in cases where a fermion is crossed from the final to the initial state. Combining the minus sign from crossing with (7), the splitting functions become positive in all cases. However, further out in the IF region, z_a or z_b may become negative, leading to a negative value for some cases in (7). We suggest that the splitting functions in those cases should be set to zero in this region. We will discuss this point further in Sections 6 and 7.

The splitting functions $\mathcal{S}$ must give the correct universal behavior in the soft and collinear limits. In the soft limit, $z_c \to 0$, the numerators must go to 1 if the flavor and helicity of the final partons a and b match those of the initial partons A and B; otherwise, the numerators must go to 0. It is easy to check that this test is satisfied.

In the collinear limits, we will insist that each antenna has the collinear behavior required in QCD. One often hears the following statement about soft and collinear

	$+++$	$++-$	$+-+$	$-++$	$--+$	$-+-$	$+--$	$---$
$g_+g_+ \to ggg$	1	y_{ac}^4	y_{ab}^4	y_{bc}^4	0	0	0	0
$g_-g_+ \to ggg$	0	0	y_{bc}^4	z_a^4	z_b^4	y_{ac}^4	0	0
$g_+g_+ \to \overline{q}qg$	-	-	$y_{ab}^3 y_{bc}$	$y_{ab} y_{bc}^3$	-	0	0	-
$g_-g_+ \to \overline{q}qg$	-	-	$y_{ab} y_{bc}^3 z_b^2$	$z_a^2 z_b^2 y_{ab} y_{bc}$	-	0	0	-
$q_-\overline{q}_+ \to qg\overline{q}$	-	-	-	$y_{ab} z_a^2$	$y_{ab} z_b^2$	-	-	-
$q_-\overline{q}_- \to qg\overline{q}$	-	-	-	-	-	y_{ab}^3	-	y_{ab}
$q_-g_- \to qgg$	-	-	-	0	y_{ac}^4	$y_{ab}^3 z_b$	-	z_a
$q_-g_+ \to qgg$	-	-	-	z_a^3	$y_{ab} z_b^3$	y_{ac}^4	-	0
$q_-g_- \to q\overline{q}q$	-	-	-	-	$y_{ab} y_{ac}^3$	$y_{ab}^2 y_{ac} z_b$	-	-
$q_-g_+ \to q\overline{q}q$	-	-	-	-	$z_a y_{ab} y_{ac} z_b^2$	$z_a y_{ab} y_{ac}^3$	-	-

Table 1: Numerator functions $\mathcal{N}(z_a, z_b, z_c)$ for the polarized $2 \to 3$ splitting functions $AB \to acb$: $\mathcal{S} = \mathcal{N}/(y_{ab} y_{ac} y_{bc})$. Each line gives a choice of AB. The labels denote the polarization of the three final particles with the radiated particle c in the center: (h_a, h_c, h_b). The empty columns are forbidden by quark chiral symmetry. By the P and C invariance of QCD, the same expressions apply after exchanging $- \leftrightarrow +$, $q \leftrightarrow \overline{q}$, or $ABacb \leftrightarrow BAbca$.

limits: In dipole splitting ($1 \to 2$ emission), each dipole has the correct collinear behavior but the correct soft behavior is obtained by combining neighboring dipoles. In antenna splitting ($2 \to 3$ emission), each antenna has the correct soft limit but the correct collinear behavior is obtained by combining neighboring antennae. However, in the large N_c limit, which we take to guide our intuition, different antennae are independent radiators with different, non-interfering, colors flowing in them. Thus, we conclude that each antenna, separately, must give collinear radiation of the form predicted by QCD. A radiating gluon belongs to two antennae, and so the total radiation collinear with that gluon will be the sum of two contributions. However, these two contributions will be identical and will simply give a factor 2 for the total emission rate. This philosophy differs from that of the ARIADNE group [6,7] and of [9]. We will discuss this point further when we compare with their results in Section 7.

To make this criterion precise, consider the limit in which c becomes collinear with a. In this limit,

$$z_c \to z \ , \qquad z_a \to (1-z) \ , \quad z_b \to 1 \ , \quad y_{ac} \to 0 \ . \tag{9}$$

The $2 \to 3$ splitting function must reduce to

$$\mathcal{S} \to \frac{1}{y_{ac}} P(z) \ , \tag{10}$$

here $P(z)$ is the relevant polarized Altarelli-Parisi splitting function. These were presented in the original Altarelli-Parisi paper [3] and are reviewed in Table 2. The

	$++$	$-+$	$+-$	$--$
$g_+ \to gg$:	$1/z(1-z)$	$(1-z)^3/z$	$z^3/(1-z)$	0
$g_+ \to q\overline{q}$:	-	$(1-z)^2$	z^2	-
$q_- \to gq$:	-	-	$(1-z)^2/z$	$1/z$
$q_- \to qg$:	-	$z^2/(1-z)$	-	$1/(1-z)$

Table 2: Polarized Altarelli-Parisi splitting functions $P(z)$ for splittings $B \to cb$. The labels denote the polarization of the two final particles with the radiated particle first: (h_c, h_b). The empty columns are forbidden by quark chiral symmetry. By the P and C invariance of QCD, the same expressions apply after exchanging $- \leftrightarrow +$ or $q \leftrightarrow \overline{q}$.

functions are normalized as in (5), and as described in the previous paragraph: We take the large N_c limit and divide by 2 where necessary to give the contribution from one QCD antenna. The denominator of (7) tends to $y_{ac}z(1-z)$ in this limit. Then it is easy to check that the numerators match correctly in all cases. The limit in which c becomes collinear with b can be checked in the same way.

When the collinear limits and the soft limit are all nonzero, there is a unique monomial of the y's and z's that gives all limits correctly. In the other cases, there is some ambiguity. In all cases, it would be desirable if the results in Table 1 could be derived directly by simple Feynman diagram computations. In the next few sections, we will present those derivations.

3 Spin-0 case

To compute the $2 \to 3$ splitting functions, we will use the following method: Write an operator that, at the leading order, creates a 2-parton state with definite helicity. Then, compute the 3-particle matrix element. This realizes in a very simple way the splitting process illustrated in Fig. 1.

To create massless quarks and antiquarks of definite helicity, we will use the appropriate chiral fermion fields. To create gluons of definite helicity, we will use the operators

$$\sigma \cdot F = \frac{1}{2}\sigma^m\overline{\sigma}^n F_{mn} \ , \qquad \overline{\sigma} \cdot F = \frac{1}{2}\overline{\sigma}^m\sigma^n F_{mn} \ , \tag{11}$$

where σ^m, $\overline{\sigma}^m$ are the 2×2 matrix entries of the Dirac matrices in a chiral basis and F_{mn} is the gluon field strength tensor. At leading order, $\sigma \cdot F$ creates a $+$ helicity gluon, and $\overline{\sigma} \cdot F$ creates a $-$ helicity gluon.

The 2-parton state g_+g_+ in the first line of Table 1 can be created from the spin-0

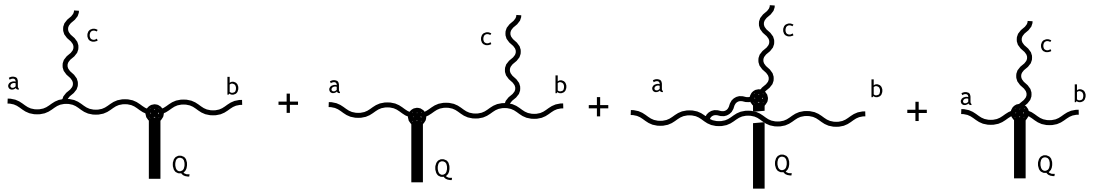

Figure 2: Feynman diagrams for the computation of the $gg \to ggg$ splitting functions.

operator

$$\mathcal{O} = \frac{1}{2}\mathrm{tr}[(\sigma \cdot F)^2] \ . \tag{12}$$

We can then compute the splitting function for this polarized initial state explicitly from the definition

$$\mathcal{S}(z_a, z_c, z_b) = Q^2 \left| \frac{\mathcal{M}(\mathcal{O} \to acb)}{\mathcal{M}(\mathcal{O} \to AB)} \right|^2 \tag{13}$$

In the next few sections, we will compute all of the splitting functions in Table 1 using this formula, with a different choice of the operator $\mathcal{O}$ for each line of the table.

To evaluate (13), we need to compute the matrix elements of $\mathcal{O}$, with total momentum Q injected, to 3-gluon final states. The result can be expressed in terms of color-ordered amplitudes. We identify the color-ordered amplitude that multiplies the color structure $\mathrm{tr}[T^a T^c T^b]$ with the splitting function. To carry out these computations, we will use the spinor product formalism. That is, instead of working with 4-vectors, we will use as our basic objects the spinor products

$$\langle ij \rangle = \overline{u}_-(i) u_+(j) \ , \qquad [ij] = \overline{u}_+(i) u_-(j) \ . \tag{14}$$

These objects obey

$$|\langle ij \rangle|^2 = |[ij]|^2 = s_{ij} \ . \tag{15}$$

Methods for QCD computations with spinor products and color-ordering are explained in [18,19]. In this notation, the matrix element for $\mathcal{O}$ to create a $g_+ g_+$ final state is

$$\langle g_+ g_+ | \, \mathcal{O} \, |0\rangle = [12]^2 \ . \tag{16}$$

The three-gluon matrix elements of the operator (12) are given by the diagrams in Fig. 2. These diagrams have already been analyzed by Dixon, Glover, and Khoze as a part of their analysis of the coupling of the Higgs boson to multi-gluon states [20]. They find

$$\mathcal{A}(\mathcal{O} \to g_+ g_+ g_+) = \frac{s_{AB}^2}{\langle ac \rangle \langle cb \rangle \langle ba \rangle}$$

$$\mathcal{A}(\mathcal{O} \to g_+ g_+ g_-) = \frac{[ac]^4}{[ac][cb][ba]}$$
$$\mathcal{A}(\mathcal{O} \to g_+ g_- g_+) = \frac{[ab]^4}{[ac][cb][ba]}$$
$$\mathcal{A}(\mathcal{O} \to g_- g_+ g_+) = \frac{[bc]^4}{[ac][cb][ba]} \tag{17}$$

and zero for the other four cases. After squaring, using (15), and dividing by the square of (16), we obtain the first line of Table 1.

One of the major points of [20] is that the results (17) belong to series of Maximally Helicity Violating (MHV) amplitudes that have a simple form for any number of gluons emitted. Actually, all of the amplitudes that we will compute in this paper are similarly simple and belong to MHV series. The use of MHV amplitudes to study antenna splitting is explored for higher-order processes in [15].

In principle, the initial state $g_+ g_+$ could also have been created by an operator of spin 2, or some higher spin. This would have led to a more complicated expression for the $2 \to 3$ splitting function, with, however, the same soft and collinear limits. This illustrates the ambiguity in the definitions of $2 \to 3$ splitting functions refered to in the introduction. The simplest results are obtained using the operator of minimal spin, and we will make that choice in all of the examples to follow.

The diagram shown in Fig. 3 gives the splitting of the two-gluon initial state to $\overline{q}qg$. We find

$$\mathcal{A}(\mathcal{O} \to \overline{q}_+ q_- g_+) = \frac{[ab]^2}{[ac]}$$
$$\mathcal{A}(\mathcal{O} \to \overline{q}_- q_+ g_+) = \frac{[cb]^2}{[ac]} \tag{18}$$

There is no splitting to a final g_-. This gives the result in the third line of the table.

The initial state $q_- \overline{q}_-$ can also be created by a spin 0 operator

$$\mathcal{O} = \overline{q}_L q_R \ . \tag{19}$$

The matrix element for this operator to create a $q_- \overline{q}_-$ final state is

$$\left\langle q_- \overline{q}_- \right| \mathcal{O} \left| 0 \right\rangle = \langle AB \rangle \ . \tag{20}$$

A straightforward calculation gives

$$\mathcal{A}(\mathcal{O} \to q_- g_+ \overline{q}_-) = \frac{\langle ab \rangle^2}{\langle ac \rangle \langle cb \rangle}$$

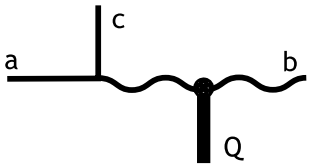

Figure 3: Feynman diagram for the computation of the $gg \to \overline{q}qg$ splitting functions.

$$\mathcal{A}(\mathcal{O} \to q_- g_- \overline{q}_-) = \frac{s_{AB}}{[ac][cb]} \tag{21}$$

These give the results shown in the sixth line of the table.

4 Spin-1 and spin-2 case

In [6], the $2 \to 3$ splitting function for $q\overline{q} \to qg\overline{q}$ was derived from the cross section for $e^+e^- \to qg\overline{q}$. From the point of view of the previous section, this corresponds to creating the 2- and 3-parton final states using the operator

$$\mathcal{O} = \overline{q}_L \gamma^m q_L \ . \tag{22}$$

To obtain a definite matrix element, we must contract this operator with a polarization vector. A convenient choice is to introduce two new massless vectors 1 and 2, such that $k_1 + k_2 = k_A + k_B$, and to choose the polarization vector to be $\epsilon^\mu = \langle 1|\gamma^\mu|2]$. This is effectively the procedure of decaying the massive vector that couples to the operator (22) into a pair of massless vectors to facilitate the analysis; this is a standard method in spinor product calculations [21]. We then recast

$$\mathcal{O} = \frac{1}{2}\overline{q}_L \gamma^m q_L \ \langle 1|\gamma_m|2] \ . \tag{23}$$

The matrix elements of (23) to a $q_-\overline{q}_+$ state is

$$\left\langle q_-\overline{q}_+ \right| \mathcal{O} \left|0\right\rangle = -\langle 1A\rangle[2B] \ . \tag{24}$$

The direction of the 1-2 system chooses the helicity of the final partons. In this case, there is only one choice, and so the amplitude vanishes when 1 is parallel to A or 2 is parallel to B. This will not always be true in our later examples. But, we will always be able to choose the desired helicity of A and B by choosing 1 parallel to B and 2 parallel to A.

The matrix elements for the operator (23) to create 3-parton final states are

$$\mathcal{A}(\mathcal{O} \to q_- g_+ \overline{q}_+) = \frac{\langle 1a\rangle^2 [12]}{\langle ac\rangle\langle cb\rangle}$$
$$\mathcal{A}(\mathcal{O} \to q_- g_- \overline{q}_+) = \frac{[2b]^2 \langle 12\rangle}{[ac][cb]} \ . \tag{25}$$

To compute the results in the fifth line of the table, we must essentially divide (25) by (24) and square the result. To do this, we need a prescription for treating the expressions $\langle 1a\rangle$ and $[2b]$ in the numerators. A treatment that is simple and becomes exact in the collinear and soft limits is to approximate a collinear with A and b collinear with B. Then identifying 1 with B and 2 with A gives

$$|\langle 1a\rangle|^2 = s_{Ba} \to z_a s_{AB} \ , \quad |\langle 1b\rangle|^2 \to 0 \ , \quad |\langle 2a\rangle|^2 \to 0 \ , |\langle 2b\rangle|^2 = s_{Ab} \to z_b s_{AB} \ , \tag{26}$$

and similarly for the conjugate products. Using this prescription, one obtains the fifth line of the table. This is a more formal version of the argument for these entries already given in Section 2.

In our calculations, we will encounter two more numerator objects that depend on 1 or 2, namely, $\langle 1c\rangle$ and $\langle 2c\rangle$. The prescription above gives

$$|\langle 1c\rangle|^2 = s_{Bc} \to (y_{bc}/z_b) s_{AB} \ , \quad |\langle 2c\rangle|^2 = s_{Ac} \to (y_{ac}/z_a) s_{AB} \ . \tag{27}$$

However, it is potentially dangerous to write factors of z_a, z_b in the denominator. We will see in Section 6 that such factors would create unphysical singularities when continued to the IF kinematics. Fortunately, we will see that $\langle 1c\rangle$ arises only in situations where there is no collinear singularity with c parallel to b. In such cases, the remaining universal singular terms—the collinear singularity with c parallel to a and the soft singularity—correspond to kinematic limits with $z_b \to 1$. A similar consideration applies to $\langle 2c\rangle$. Thus, we choose, instead of using (27), to evaluate these quantities as

$$|\langle 1c\rangle|^2 = s_{Bc} \to y_{bc} s_{AB} \ , \quad |\langle 2c\rangle|^2 = s_{Ac} \to y_{ac} s_{AB} \ . \tag{28}$$

This gives an incorrect shape in a region where a and b are collinear, but, hopefully, we will not use the $AB \to acb$ splitting function to evaluate the rate to fill this region of phase space.

Another choice for evaluating $\langle 1c\rangle$ and $\langle 2c\rangle$ is to replace both expressions by z_c. However, the spinor product $\langle 1c\rangle$ vanishes in the bc collinear limit but not in the ac collinear limit, and conversely for $\langle 2c\rangle$, so this choice does not give the universal singularities correctly.

We now apply this formalism to compute the second and fourth lines of Table 1, associated with the g_-g_+ antenna. This antenna is created by the spin-2 operator $\mathrm{tr}[\gamma^m(\overline{\sigma}\cdot F)\gamma^n(\sigma\cdot F)]$. To make a definite calculation, we need a spin-2 polarization vector. An appropriate choice can be found by introducing the massless vectors 1 and 2 as above and writing

$$\epsilon^{mn} = \langle 1|\gamma^m|2]\ \langle 1|\gamma^n|2]\ . \tag{29}$$

This effectively decays the masive spin-2 particle into two massless spinors. This method was introduced in [22] to compute the relevant amplitudes for the emission of massive gravitons at high-energy colliders.

With this prescription, we generate the g_-g_+ antenna using the operator

$$\mathcal{O} = \frac{1}{4}\mathrm{tr}[\gamma^m(\overline{\sigma}\cdot F)\gamma^n(\sigma\cdot F)]\langle 1|\gamma_m|2]\langle 1|\gamma_n|2] \tag{30}$$

The matrix element of this operator that creates the 2-parton dipole is

$$\langle g_-g_+|\,\mathcal{O}\,|0\rangle = \langle 1A\rangle^2[2B]^2\ . \tag{31}$$

To obtain the correct initial polarizations, we take $1 = B$, $2 = A$ as before. The matrix elements to the possible 3-parton final states are

$$\begin{aligned}
\mathcal{A}(\mathcal{O}\to g_+g_+g_+) &= 0\\
\mathcal{A}(\mathcal{O}\to g_+g_+g_-) &= \frac{\langle 1b\rangle^4[12]^2}{\langle ab\rangle\langle ac\rangle\langle cb\rangle}\\
\mathcal{A}(\mathcal{O}\to g_+g_-g_+) &= \frac{\langle 1c\rangle^4[12]^2}{\langle ab\rangle\langle ac\rangle\langle cb\rangle}\\
\mathcal{A}(\mathcal{O}\to g_-g_+g_+) &= \frac{\langle 1a\rangle^4[12]^2}{\langle ab\rangle\langle ac\rangle\langle cb\rangle}\ ,
\end{aligned} \tag{32}$$

and the conjugates with $1\leftrightarrow 2$ for the other four combinations. Applying the reductions (26), (27), we find the results given in the second line of the table.

The nonzero matrix elements of this operator to $\overline{q}qg$ final states are

$$\begin{aligned}
\mathcal{A}(\mathcal{O}\to \overline{q}_+q_-g_+) &= \frac{\langle 1c\rangle^2[2b]^2}{[ac]}\\
\mathcal{A}(\mathcal{O}\to \overline{q}_-q_+g_+) &= \frac{\langle 1a\rangle^2[2b]^2}{[ac]}\ .
\end{aligned} \tag{33}$$

The same reduction process gives the results in the fourth line of the table.

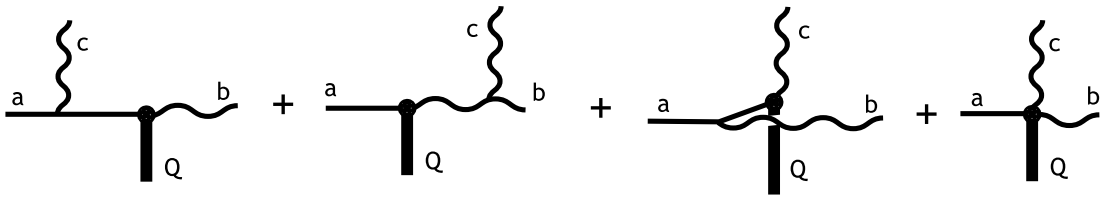

Figure 4: Feynman diagrams for the computation of the $qg \to qgg$ splitting functions.

5 Spin-$\frac{1}{2}$ and spin-$\frac{3}{2}$ cases

The cases of quark-gluon antennae can be treated in the same way. There is one additional subtlety. In QCD, quarks are color triplets and gluons are color octets, so a quark-gluon operator carries net color. This means that the matrix element for gluon emission from a quark-gluon operator is not gauge-invariant unless we allow the gluon also to be emitted from the initial state. This makes it unclear how to define a quark-gluon antenna.

We resolve this problem with the following prescription: We consider the quarks to be color octet particles like the gluons. Then, as in the previous sections, we extract the color-ordered contribution corresponding to emission from the antenna. In the limit of large N_c, the various antennae in a process radiate independently. The diagrams contributing to a quark-gluon antenna in this prescription are shown in Fig. 4. The third diagram, with an intermediate quark line, does not appear in QCD. However, it does nicely provide the missing piece that makes this sum of digrams gauge-invariant without radiation from the initial state.

With this understanding, we proceed as above. We can generate the $q_- g_-$ antenna using the operator $\overline{q}_L(\overline{\sigma} \cdot F)$. The polarization spinor can be built by introducing massless spinors 1 and 2 as above and taking $|2\rangle$ to be this spinor. Then

$$\mathcal{O} = -i\overline{q}_L(\overline{\sigma} \cdot F)\,|2\rangle \ . \tag{34}$$

The matrix element of this operator that creates the 2-parton dipole is

$$\langle q_- g_-|\,\mathcal{O}\,|0\rangle = \langle AB\rangle[B2] \ . \tag{35}$$

To obtain the correct initial polarizations, we take $1 = B$, $2 = A$.

The matrix elements to the possible 3-parton final states are

$$\mathcal{A}(\mathcal{O} \to q_- g_+ g_+) = 0$$

$$\mathcal{A}(\mathcal{O} \to q_- g_- g_+) = \frac{\langle ac\rangle^3\langle 2c\rangle}{\langle ab\rangle\langle ac\rangle\langle cb\rangle}$$
$$\mathcal{A}(\mathcal{O} \to q_- g_+ g_-) = \frac{\langle ab\rangle^3\langle 2b\rangle}{\langle ab\rangle\langle ac\rangle\langle cb\rangle}$$
$$\mathcal{A}(\mathcal{O} \to q_- g_- g_-) = \frac{s_{AB}\langle 12\rangle[1a]}{[ab][ac][cb]} \ . \tag{36}$$

Applying the reductions (26), (27), we find the results given in the seventh line of the table.

The nonzero matrix elements of this operator to $q\bar{q}q$ final states are

$$\mathcal{A}(\mathcal{O} \to q_- \bar{q}_- q_+) = \frac{\langle ac\rangle\langle 2c\rangle}{\langle cb\rangle}$$
$$\mathcal{A}(\mathcal{O} \to q_- \bar{q}_+ q_-) = -\frac{\langle ab\rangle\langle 2b\rangle}{\langle cb\rangle} \ . \tag{37}$$

The same reduction process gives the results in the ninth line of the table.

We generate the $q_- g_+$ antenna using the spin-$\frac{3}{2}$ operator $\bar{q}_L\gamma^m(\sigma\cdot F)$. This is essentially the supersymmetry current of the system of gluons and color octet fermions. The polarization spinor can be built by introducing massless spinors 1 and 2 as above:

$$\mathcal{O} = i\bar{q}_L\gamma^m(\sigma\cdot F)\,2]\langle 1|\gamma_m|2] \ . \tag{38}$$

The matrix element of this operator that creates the 2-parton dipole is

$$\langle q_- g_+|\,\mathcal{O}\,|0\rangle = \langle 1A\rangle[2B]^2 \ . \tag{39}$$

To obtain the correct initial polarizations, we again take $1 = B$, $2 = A$.

The matrix elements to the possible 3-parton final states are

$$\mathcal{A}(\mathcal{O} \to q_- g_+ g_+) = \frac{\langle 1a\rangle^3[12]^2}{\langle ab\rangle\langle ac\rangle\langle cb\rangle}$$
$$\mathcal{A}(\mathcal{O} \to q_- g_- g_+) = \frac{\langle ab\rangle[2b]^3\langle 12\rangle}{[ab][ac][cb]}$$
$$\mathcal{A}(\mathcal{O} \to q_- g_+ g_-) = \frac{\langle ac\rangle[2c]^3\langle 12\rangle}{[ab][ac][cb]}$$
$$\mathcal{A}(\mathcal{O} \to q_- g_- g_-) = 0 \ . \tag{40}$$

Applying the reductions (26), (27), we find the results given in the eighth line of the table.

The nonzero matrix elements of this operator to $q\bar{q}q$ final states are

$$\mathcal{A}(\mathcal{O} \to q_-\overline{q}_-q_+) = \frac{\langle 1a\rangle[2b]^2}{[cb]}$$
$$\mathcal{A}(\mathcal{O} \to q_-\overline{q}_+q_-) = -\frac{\langle 1a\rangle[2c]^2}{[cb]} \ . \tag{41}$$

The same reduction process gives the results in the tenth line of the table.

6 Initial-state showers

The Feynman diagram computations that we have done to find the antenna splitting functions for FF splittings can also be applied, by crossing, to IF and II splittings. The expressions in Table 1 are given in terms of invariant quantities that are unchanged under crossing. Thus, we can use the expressions in this table directly in other channels. At worst, a change of the overall sign is required in some cases. In this section, we will clarify this statement by analyzing the kinematics of IF and II splittings in the same variables as those used in Section 2 for FF splittings. In all cases, the kinematics is done for all massless partons only. The kinematic discussion in this section is similar to that presented in [23].

To begin, we will formalize some of the results quoted in Section 2 for the FF region. The cross section for a process $X \to acb$ is

$$\sigma(X \to acb) = \frac{1}{\Phi_X}\frac{s}{128\pi^3}\int dz_a dz_b |\mathcal{M}(X \to acb)|^2 \ , \tag{42}$$

where Φ_X is the flux factor. Polarization and color indices have been suppressed. The left-hand side has been integrated over the orientation of the final state system but is otherwise exact. To write an expression involving the antenna splitting function, we approximate

$$\mathcal{M}(X \to acb) \approx \mathcal{M}(X \to AB) \cdot gT \cdot \frac{\mathcal{M}(\mathcal{O} \to acb)}{\mathcal{M}(\mathcal{O} \to AB)} \ , \tag{43}$$

where $\mathcal{O}$ is the operator used in Sections 3–5 to represent the state AB. The factor gT is the QCD coupling and color matrix; after squaring and summing over colors, this becomes $4\pi\alpha_s N_c$. The splitting function is defined by (13),

$$\mathcal{S}(z_a, z_c, z_b) = s_{AB}\left|\frac{\mathcal{M}(\mathcal{O} \to acb)}{\mathcal{M}(\mathcal{O} \to AB)}\right|^2 \tag{44}$$

Then

$$\sigma(X \to acb) \approx \sigma(X \to AB) \cdot \frac{\alpha_s N_c}{4\pi} \int dz_a dz_b \mathcal{S}(z_a, z_c, z_b) \ . \tag{45}$$

It is important to note that, in this formula or in (43), the vectors k_A and k_B are introduced as part of the approximation. They can be defined in any way that is consistent with the requirements that k_A and k_B are lightlike, $k_A + k_B = Q$, and k_A and k_B become parallel to k_a and k_b, respectively, in the soft and collinear limits.

The logic of this derivation extends straightforwardly to the IF and II regions. The major change is that, in these cases, we need to introduce initial hadrons from which the initial partons are extracted.

Consider first the IF case. The cross section for a proton of momentum P to scatter from a color-singlet system X transferring momentum Q to create a 2-parton system cb is

$$\sigma(pX \to cb) = \int dx_a f(x_a) \ \frac{1}{\Phi_{aX}} \frac{1}{16\pi} \int d\cos\theta_* \ |\mathcal{M}(aX \to cb)|^2 \ , \tag{46}$$

where $\cos\theta_*$ is the scattering angle in the cb center of mass system. We will approximate this formula using the expression analogous to (43)

$$\mathcal{M}(aX \to cb) \approx \mathcal{M}(AX \to B) \cdot gT \cdot \frac{\mathcal{M}(a\mathcal{O} \to cb)}{\mathcal{M}(A\mathcal{O} \to B)} \ . \tag{47}$$

Then the splitting function is defined by the same expression $\mathcal{S}$ as in (44), but now analytically continued into the new kinematic region. If a fermion line is crossed from the final to the initial state, an extra factor (-1) should be included.

The decomposition of the amplitude is illustrated in Fig. 5(a). The kinematics can be described by variables y_{ij} and z_i obeying the relations (1) to (4). However, the vectors k_A, k_a now have negative timelike component, and the vector $Q = k_A + k_B = k_a + k_b + k_c$ is spacelike, $Q^2 = s_{AB} < 0$. The phase space for this region covers the quadrilateral shown in Fig. 5(b). The region of integration is infinite, since z_a can become very large, but the integral is cut of at large z_a by the parton distribution function. The line $z_a > 1$, $z_b = 1$ corresponds to the region of initial state radiation, c parallel to a. The line $z_a = 1$, $0 < z_b < 1$ corresponds to the region of final state radiation, c parallel to b. The line $z_a + z_b = 1$ corresponds to b parallel to a, that is, b as initial state radiation from the primary a. An antenna shower should give an accurate description of the dynamics in the two regions $|y_{ac}| < |y_{bc}| < 1$, $|y_{bc}| < |y_{ac}| < |y_{ab}|$ that are shaded in the figure. The new constraint $|y_{bc}| < 1$ is just $|s_{bc}| < |Q^2|$, which is stronger than the constraint that this invariant is less than $|s_{ab}|$.

To decompose (46) into an appropriate form, we choose p_A and p_B and then change variables. Let p_A be chosen in the direction of p_a, so that $p_a = z_a p_A$, $z_a > 1$. Then

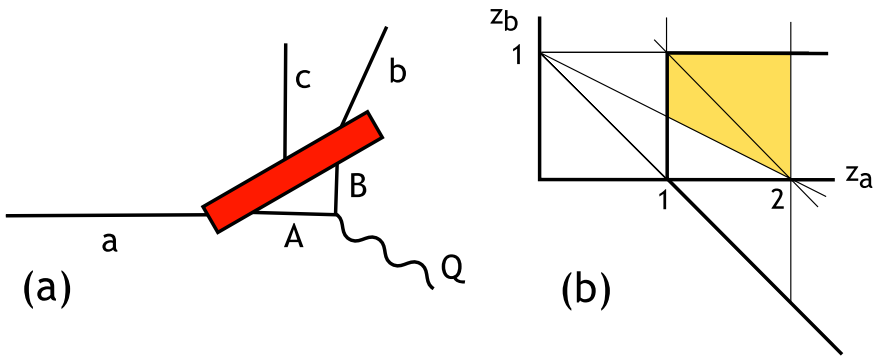

Figure 5: (a) Kinematics of $2 \to 3$ splitting in the initial-final (IF) case. (b) Phase space for $2 \to 3$ splitting in the IF case. The eight regions corresponding to different orderings of $|s_{ab}|$, $|s_{ac}|$, s_{bc}, $|Q^2|$ are shown. The region that should be well described by an antenna splitting $AB \to acb$ is shaded.

$p_B = Q - p_A$. We have

$$p_a = x_a P \ , \quad p_A = x_A P \ , \quad \text{so} \quad x_a = z_a x_A \ , \tag{48}$$

with x_A having the definite value $x_A = -Q^2/2P \cdot Q$ associated with scattering a massless particle from a local current. For the reaction $aQ \to bc$, $s + t + u = Q^2$, so $t + u = Q^2 - s = Q^2 z_a$. Then

$$t = Q^2(1 - z_b) = \frac{1}{2} Q^2 z_a (1 - \cos\theta_*) \tag{49}$$

Using these formulae, we can change variables from $(x_a, \cos\theta_*)$ to (z_a, z_b). The Jacobian of this transformation is

$$J = \frac{\partial(x_a, \cos\theta_*)}{\partial(z_a, z_b)} = \frac{2x_A}{z_a} \tag{50}$$

Thus,

$$\sigma(pX \to cb) = \int \frac{dz_a}{z_a^2} \int dz_b \int dx_A x_A f(z_a x_A)\ \delta(x_A + Q^2/2P \cdot Q) \cdot \frac{1}{\Phi_{AX}} \frac{1}{8\pi} |\mathcal{M}(aX \to cb)|^2 \ . \tag{51}$$

This is an exact rewriting of (46). Now apply the approximation (47) and group terms to form

$$\sigma(AX \to B) = \frac{1}{\Phi_{AX}} 2\pi\delta(Q^2 + x_A 2P \cdot Q) |\mathcal{M}(AX \to B)|^2 \ . \tag{52}$$

Then

$$\sigma(pX \to cb) \approx \int \frac{dz_a}{z_a^2} \int dz_b \int dx_A f(z_a x_A) \sigma(AX \to B) \cdot \frac{\alpha_s N_c}{4\pi} \mathcal{S}(z_a, z_c, z_b) \ . \tag{53}$$

As an example, consider using this formula to describe initial-state gluon radiation in deep inelastic scattering from a quark. The total gluon emission is given by the sum of the two polarized splitting functions in the fifth line of Table 1, equal to

$$\sum \mathcal{S} = \left| \frac{z_a^2 + z_b^2}{y_{ac} y_{cb}} \right| \ , \tag{54}$$

We have supplied an extra minus sign because we cross a fermion. In the region of initial state radiation, $z_a = 1/w$, $z_b \approx 1$, $y_{ac} = (1 - z_b)$, $y_{bc} = (1 - 1/w)$. Then, setting

$$\int dz_b \frac{1}{1 - z_b} = \log \frac{Q^2}{\mu^2} \ , \tag{55}$$

we obtain

$$\sigma(pX \to cb) \approx \int dx_A \int \frac{dw}{w} f(\frac{x_A}{w}) \, \sigma(AX \to B) \cdot \frac{\alpha_s N_c}{4\pi} \frac{1 + w^2}{(1 - w)} \log \frac{Q^2}{\mu^2} \ , \tag{56}$$

which is correct.

For the II case, we begin from the formula for two protons of momentum P_A, P_B to produce a color-singlet system of momentum Q plus a massless parton c,

$$\sigma(pp \to cX) = \int dx_a \int dx_b f(x_a) f(x_b) \ \frac{1}{2 s_{ab}} \frac{1}{16\pi} \int d\cos\theta_* \frac{2 p_*}{\sqrt{s_{ab}}} \, |\mathcal{M}(ab \to cX)|^2 \ , \tag{57}$$

where $\cos\theta_*$ and p_* are the scattering angle and the momentum in the cX center of mass frame.

The decomposition of the amplitude is illustrated in Fig. 6(a). The kinematics can again be described by variables y_{ij} and z_i obeying the relations (1) to (4). Now the vectors k_A, k_a k_B, k_b have negative timelike component, and the vector $Q = k_A + k_B = k_a + k_b + k_c$ is also negative timelike, with $Q^2 > 0$. The phase space for this region covers the quadrant shown in Fig. 5(b), with $z_a, z_b > 1$. Again, the region of integration is infinite, but the integral is cut off by the behavior of the parton distribution functions. The line $z_a > 1$, $z_b = 1$ corresponds to the region of initial state radiation with c parallel to a. The line $z_a = 1$, $z_b > 1$ corresponds to the region of initial state radiation with c parallel to b. An antenna shower should give an accurate description of the dynamics in the two regions $|y_{ac}| < |y_{bc}| < 1$, $|y_{bc}| < |y_{ac}| < 1$ that are shaded in the figure. Again, the limit 1 here corresponds to

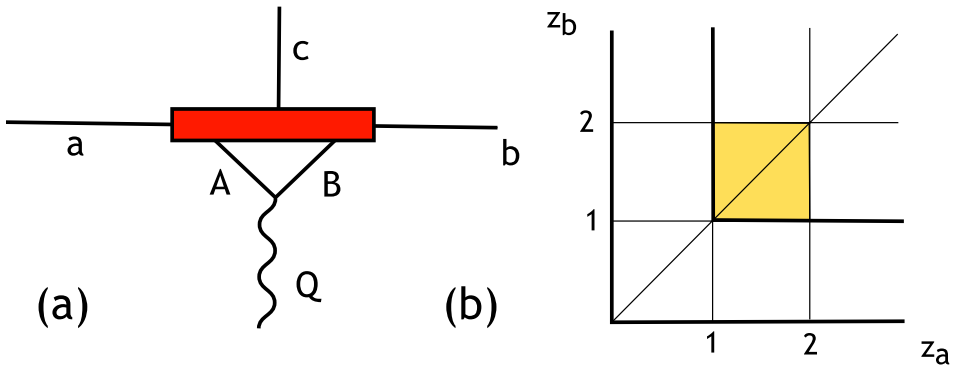

Figure 6: (a) Kinematics of $2 \to 3$ splitting in the initial state (II) case. (b) Phase space for $2 \to 3$ splitting in the II case. The six regions corresponding to different orderings of $|s_{ac}|$, $|s_{bc}|$, $|Q^2|$ are shown. The region that should be well described by an antenna splitting $AB \to acb$ is shaded.

constraints $|s_{ac}|, |s_{bc}| < |Q^2|$, which are stronger than the constraints that these two invariants are less than $|s_{ab}|$.

In the $ab \to cX$ process, the system X must recoil with some nonzero transverse momentum. Thus, it is not possible to choose k_A and k_B to be parallel to k_a, k_b. The invariants for the $ab \to cX$ scattering process satisfy $s + t + u = Q^2$. Since $t = Q^2(1 - z_b)$, $u = Q^2(1 - z_a)$, this means that $s = Q^2(z_a + z_b - 1)$. Alternatively, $s = x_a x_b \cdot 2P_A \cdot P_B$. We would like to choose the longitudinal fractions of A and B, x_A and x_B, to satisfy the relation

$$x_A x_B \cdot 2P_A \cdot P_B = Q^2 \ . \tag{58}$$

To make this possible, we must write

$$x_a = z_a x_A \mathcal{C} \ , \qquad x_b = z_b x_B \mathcal{C} \ , \tag{59}$$

with [24]

$$\mathcal{C}^2 = \frac{z_a + z_b - 1}{z_a z_b} \tag{60}$$

The function $\mathcal{C}(z_a, z_b)$ approaches 1 when *either* z_a or z_b goes to 1; that is $\mathcal{C} \approx 1$ in both collinear regions.

Also, $t + u = Q^2(2 - z_a - z_b) = Q^2 z_c$, so

$$t = Q^2(1 - z_b) = \frac{1}{2} Q^2 z_c (1 - \cos\theta_*) \ . \tag{61}$$

We can now use (59) and (61) to change variables from $(x_a, x_b, \cos\theta_*)$ to (x_A, z_a, z_b), holding x_B fixed at the value $x_B = Q^2/x_A 2P_A \cdot P_B$. The Jacobian of this transformation is

$$J = \frac{\partial(x_a, x_b, \cos\theta_*)}{\partial(x_A, z_a, z_b)} = \frac{2x_B}{z_c} = x_B \frac{Q^2}{s_{ab}} \frac{\sqrt{s_{ab}}}{p_*} \ . \tag{62}$$

Then

$$\sigma(pp \to cX) = \int \frac{dz_a}{z_a^2} \frac{dz_b}{z_b^2} \frac{1}{\mathcal{C}^4} \int dx_A dx_B \, f(z_a x_A \mathcal{C}) f(z_b x_B \mathcal{C}) \ x_B \delta(x_B - Q^2/x_A 2P_A \cdot P_B) \cdot \frac{1}{s_{AB}} \frac{1}{8\pi} |\mathcal{M}(aX \to cb)|^2 \ . \tag{63}$$

This is an exact rewriting of (57). Now apply the approximation analogous to (43) or (47) and group terms to form

$$\sigma(AB \to X) = \frac{1}{2s_{AB}} 2\pi\delta(Q^2 - x_A x_B 2P_A \cdot P_B) |\mathcal{M}(AX \to B)|^2 \ . \tag{64}$$

This gives, finally,

$$\sigma(pp \to cX) \approx \int \frac{dz_a}{z_a^2} \frac{dz_b}{z_b^2} \frac{1}{\mathcal{C}^4} \int dx_A dx_B \, f(z_a x_A \mathcal{C}) f(z_b x_B \mathcal{C}) \sigma(AB \to X) \cdot \frac{\alpha_s N_c}{4\pi} \mathcal{S}(z_a, z_c, z_b) \ . \tag{65}$$

To test this formula, consider the case of $q\bar{q}$ annihilation with the emission of a gluon collinear with the quark a. The sum of polarized splitting functions for this case is again (54). In the collinear region of interest, $z_a = 1/w$, $z_b \approx 1$. Repeating the step that led to (56), we find

$$\sigma(pp \to cX) \approx \int dx_A dx_B \int \frac{dw}{w} f(\frac{x_A}{w}) f(x_B) \, \sigma(AB \to X) \cdot \frac{\alpha_s N_c}{4\pi} \frac{1 + w^2}{(1 - w)} \log \frac{Q^2}{\mu^2} \ , \tag{66}$$

which is the correct limit.

7 Comparison to previous results

In the Introduction, we made reference to a number of previous definitions of the antenna splitting functions. We noted that these definitions agree, as they must, in the singular soft and collinear limits. However, these prescriptions differ widely away from the boundaries of phase space. In this section, we will compare our prescription to those of ARIADNE [6,7] and Gehrmann-De Ridder, *et al.* [16].

We will make this comparison over the natural phase space discussed in the previous section–the entire (z_a, z_b) plane above the line $z_a + z_b = 1$. In order to describe antenna showers for initial- as well as final-state emissions, the splitting functions should extend into the region $z_a, z_b > 1$. Depending on the details of how the shower is constructed, their use might be restricted to a polygon around $z_a = z_b = 1$, or the expressions might be used for arbitrarily large values of z_a and z_b.

We note again that the IF regions include the lines $z_a = 0$ and $z_b = 0$. Expressions for the splitting functions that are well-behaved near $z_a = z_b = 1$ can possibly have a singularity on this line, though such a singularity in the middle of the phase space would be unphysical. We used this criterion in Section 4 to exclude factors of $1/z_a$ and $1/z_b$ from appearing in (28). The antenna functions of Duhr and Maltoni [15] are typically singular along this line and so cannot be used in parton shower models in all regions.

The ARIADNE and Gehrmann-De Ridder antenna functions give expressions summed over final polarizations. To compare our splitting functions to these, we must sum over a row in Table 1. Our summed expressions are independent of the initial polarization in the soft and collinear limits, but they depend on the polarizations of A and B in the interior of the (z_a, z_b) space. The comparison to our expressions thus also reveals where this dependence on polarization is an important effect.

There is another issue when comparing our results to those of ARIADNE and Gehrmann-De Ridder, *et al.*, that must be resolved. Our antenna functions are defined for processes with definite helicity. We wish to interpret them as probabilities over all of phase space. In particular, this means that the antenna functions must be positive. In the FF region of phase space, our functions are manifestly positive. In the IF and II regions in the vicinity of the point $z_a = z_b = 1$, the expression (7) can be negative in some cases, but the minus sign is always compensated by a minus sign from crossing a fermion from the final to the initial state. In these cases, it suffices to define the splitting function as the absolute value of (7). However, some of our expressions also change sign in the IF region as one crosses the line where z_a or z_b equals zero. We regard this behavior as unphysical, and we will resolve the problem by setting the antenna functions for the specific helicities in which it occurs to zero on the far side of the lines $z_a = 0$ or $z_b = 0$. The expressions for the remaining helicities generally give a positive continuation of the splitting function to the regions where z_a or z_b are negative. We note that the regions where z_a and z_b are negative lie outside the part of the IF regions most important for a parton shower as indicated in Fig. 5.

For the ARIADNE and Gehrmann-De Ridder antenna functions, the expressions given are summed over spins, and the individual pieces are not independent of one another. The full terms, with their appropriate signs after analytic continuation, are needed to reproduce the Altarelli-Parisi limits. If, as sometimes happens, these

expressions become negative, this must be fixed in the expression as a whole.

The first antenna splitting functions were put forward by the ARIADNE group [6]. Their approach started from the spin-averaged cross section for the simple splitting process $q\bar{q} \to qg\bar{q}$ in e^+e^- annihilation. They then guessed the expressions for the $qg \to qgg$ and $gg \to ggg$ splittings, so that these would have a similar form to the $q\bar{q} \to qg\bar{q}$ case,

$$\mathcal{S} = \frac{z_a^{n_a} + z_b^{n_b}}{y_{ac} y_{bc}} \ , \tag{67}$$

where $n_a, n_b = 2$ for emission from a quark and 3 for emission from a gluon.

Our philosophy, explained in Section 2, is that each individual antenna should reproduce the collinear limit predicted by QCD. These expressions are symmetric under interchange of identical particles, while (67) does not have this property, so we would obtain the complete splitting function by symmetrizing (67). This gives

$$\begin{aligned}
q\bar{q} \text{ antenna:} \quad & \mathcal{S} = \frac{z_a^2 + z_b^2}{y_{ac} y_{bc}} \ , \\
gg \text{ antenna:} \quad & \mathcal{S} = \frac{z_a^3 + z_b^3}{y_{ac} y_{bc}} + \frac{z_a^3 + z_c^3}{y_{ab} y_{bc}} + \frac{z_b^3 + z_c^3}{y_{ab} y_{ac}} \ , \\
qg \text{ antenna:} \quad & \mathcal{S} = \frac{z_a^2 + z_b^3}{y_{ac} y_{bc}} + \frac{z_a^2 + z_c^3}{y_{ab} y_{bc}} \ .
\end{aligned} \tag{68}$$

The summed terms are each positive in the FF kinematic region. To obtain the ARIADNE splitting functions in the other regions, we analytically continue these formulae into the regions where z_a or z_b is greater than 1.

We are now in a position to compare the ARIADNE function to our proposal. For the $q\bar{q}$ antenna, the expression above coincides with the sum of row 5 of Table 1. For the gg and gq cases, the ratio of the above ARIADNE functions to those defined in Table 1 are illustrated in Figs. 7, 8, and 9. The notation in the figures is the following: Each figure represents the ratio of the ARIADNE splitting function to our results for a specific initial set of polarized partons, summed over final state polarizations. The ratio goes to 1 on the lines $z_a = 1$ and $z_b = 1$, which correspond to the collinear limits. Away from these lines, the contours on which the ratios are 1.2, 1.5, 2.0, 3.0, and 5.0 (toward the + symbol), and the inverses of these numbers (toward the − symbol) are shown. The qg antenna function are asymmetric between partons a and b. The IF region in the lower right is that in which the quark is in the intial state and the gluon is in the final state. The IF region in the upper left is that in which the gluon is in the initial state and the quark remains in the final state.

The ARIADNE authors gave a different interpretation to the formulae (68). They took the philosophy that the collinear limit need not result from a single antenna but

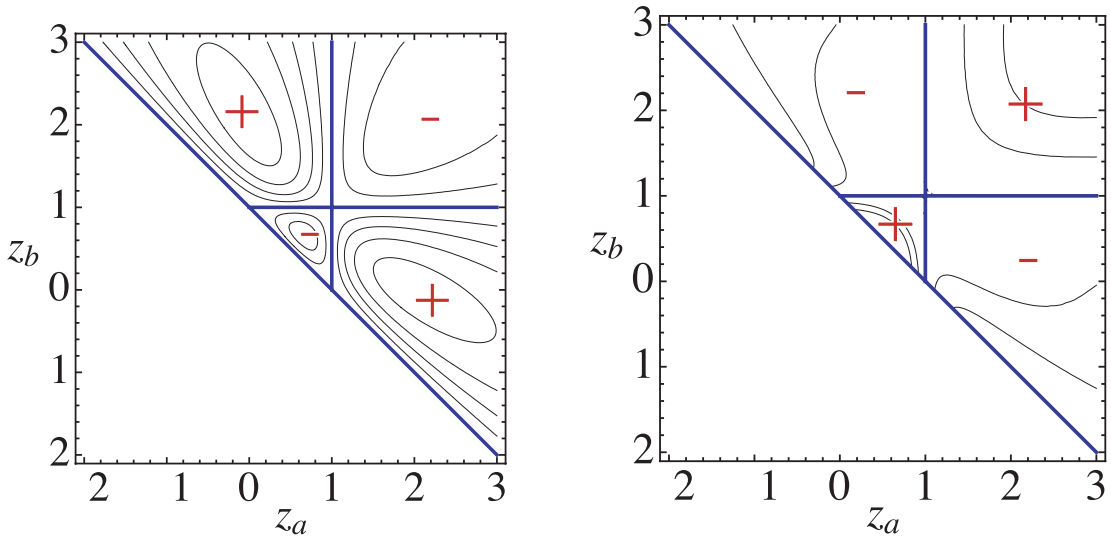

Figure 7: Visualization of the ratio of the ARIADNE antenna function to our antenna functions for the processes $gg \to ggg$. The figures on the left and right are the comparison of the ARIADNE antenna function to our spin-summed antenna functions from row 1 and row 2 in Table 1, respectively. The boundaries of phase space for the different kinematic regions are marked in blue. The contours are plotted at ratios of 1.2, 1.5, 2.0, 3.0, and 5.0, with + indicating a region in which the ratio is greater than 1.

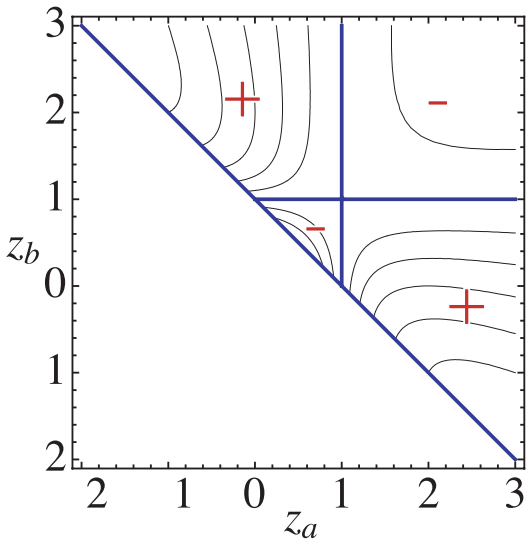

Figure 8: Visualization of the ratio of the ARIADNE antenna function to our antenna function for the process $q_-\bar{q}_- \to qg\bar{q}$. Our antenna function for the process $q_-\bar{q}_+ \to qg\bar{q}$ coincides with the ARIADNE result and so is not included. The notation is as in Fig. 7.

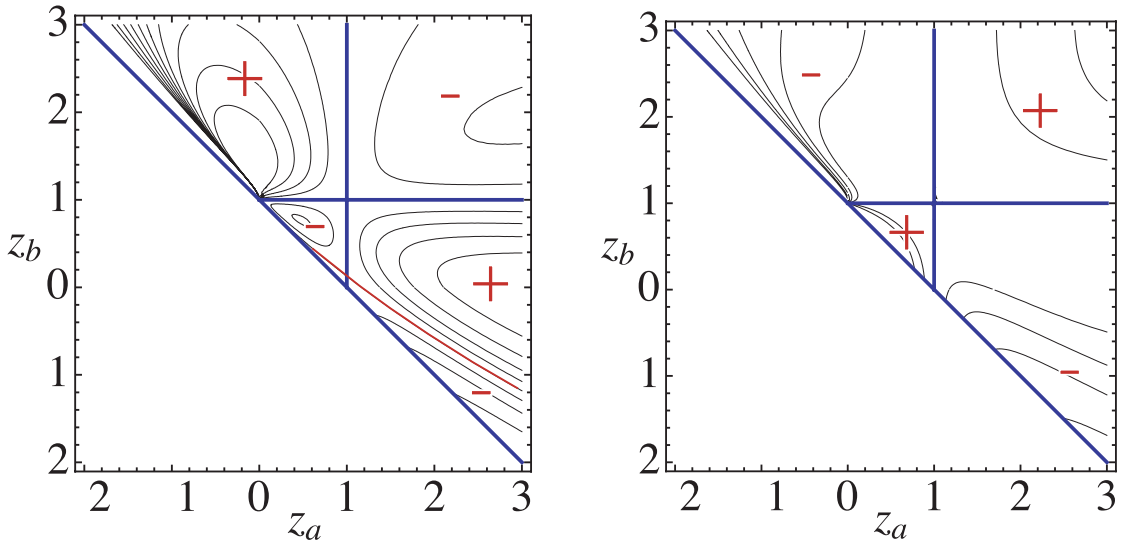

Figure 9: Visualization of the ratio of the ARIADNE antenna function to our antenna functions for the processes $qg \to qgg$. The figures on the left and right are the comparison of the ARIADNE antenna function to our spin-summed antenna functions from row 7 and row 8 in Table 1, respectively. The notation is as in Fig. 7.

rather should be the result of summing over the possible antennae that would lead to a specific final state. A three gluon final state could result from any pair of the gluons radiating the third and so should be the sum of three antennae. Then the second line of (68) would be interpretated as the sum over these three antennae. This is a reasonable point of view for the FF kinematics considered in [6]. However, in the IF and II regions, at least one of the z_i will be negative and so some of the terms in the last two lines of (68) will become negative. Such terms cannot be interpreted as independent radiators, each emittting a gluon with positive probability. It is tempting to revise the formula in (68) by taking the absolute values of the negative terms. However, one can readily check that no such prescription gives the correct Altarelli-Parisi limit along the lines $z_a = 1$ and $z_b = 1$ at the boundaries of the IF and II regions. Thus, we believe, the ARIADNE formulae can be used in the IF and II regions only by using the formulae (68) as written and accepting that some negative signs will appear [25].

Gehrmann-De Ridder, Gehrmann and Glover [16] studied $2 \to 3$ splitting from Feynman diagrams to develop an antenna subtraction program for NNLO calculations. In doing so, they were able to extract unpolarized antenna functions for the processes $gg \to ggg$, $qg \to qgg$ and $qg \to q\bar{q}q$. To calculate the gluon-gluon antenna function, they used the effective Higgs coupling to gluons

$$\mathcal{L} = -\frac{\lambda}{4} h F^{\mu\nu} F_{\mu\nu}. \tag{69}$$

This is essentially the same procedure that we used in Section 3, and it yields the same result as the sum of row 1 in Table 1. In our language, their antenna function for the gluon-gluon dipole is [26]

$$\mathcal{S} = \frac{y_{ac}^2 + y_{bc}^2 + y_{ab}^2 + y_{ac}^2 y_{bc}^2 + y_{ab}^2 y_{bc}^2 + y_{ab}^2 y_{ac}^2}{y_{ab} y_{ac} y_{bc}} + 4 \ . \tag{70}$$

The comparison of this antenna function to the sum of row 2 of Table 1 is illustrated in Fig. 10.

This splitting function for $gg \to ggg$ is, however, not precisely the form of the splitting function that is used in the VINCIA parton shower [8]. They use the 'global' form of the Gehrmann-De Ridder antenna function, which in our language is

$$\mathcal{S} = \frac{1}{2} \left[\frac{2y_{ab}^2 + y_{ab}^2 y_{ac}^2 + y_{ab}^2 y_{bc}^2}{y_{ab} y_{ac} y_{bc}} + \frac{8}{3} \right]. \tag{71}$$

To implement this antenna function, a similar procedure is used as with the ARIADNE antenna functions. That is, emissions from overlapping antenna are summed. When the three antennae contributing to $gg \to ggg$ are summed together, one recovers the result (70). This prescription. works well in the FF kinematics. However, as

in the ARIADNE case, it might require negative splitting functions for some antennae in the IF and II kinematics.

To construct the antenna functions involving quarks, Gerhmann-De Ridder, *et al.*, calculated the decay of a neutralino χ to a gluon and a gluino ψ through the effective operator

$$\mathcal{L} = i\eta\overline{\psi}\sigma^{\mu\nu}\chi F_{\mu\nu} + \text{h.c.} \tag{72}$$

This is a similar procedure to the one that we used in Section 4 in that octet fermions were utilized to eliminate any color in the initial state. However, due to our choices (26) and (28) for handling ambiguous momentum products, our antenna functions differ from theirs. In our language, their antenna functions involving quarks are

$$\begin{aligned} qg \to qgg: \;\; \mathcal{S} &= \frac{2y_{ab}^2 + 2y_{ac}^2 + y_{ab}y_{bc}^2 + y_{ac}y_{bc}^2 + 2y_{ac}^2y_{ab}^2}{y_{ab}y_{ac}y_{bc}} + 2 + 2y_{ac} + 2y_{ab} \;, \\ qg \to q\bar{q}q: \;\; \mathcal{S} &= \frac{(y_{ac}+y_{ab})^2 y_{ac}y_{ab} - 2y_{ac}^2y_{ab}^2}{y_{ab}y_{ac}y_{bc}} + y_{ab} + y_{ac} \;. \end{aligned} \tag{73}$$

The comparison to our antenna functions is illustrated in Figs. 11 and 12.

We see in the figures that our antenna functions have a substantial dependence on the initial-state helicities that is not captured in the Gehrmann-De Ridder functions. This dependence is actually strongest in the FF region, though it is present in all regions. As with the ARIADNE antenna functions, the Gehrmann-De Ridder functions can become negative in some regions. In fact, the functions involving quarks are negative in a substantial part of the left-hand IF kinematic region. These regions are not directly visible in the comparison plots Figs. 11 and 12, since our contours take only positive values. On the other hand, our expressions also have problems in this region. Our prescription of setting negative splitting functions equal to zero sets the entire splitting function to zero to the left of the $z_a = 0$ axis in the right-hand plot in Fig. 12.

In summary, we have shown that the antenna splitting functions represented by (7) and Table 1 give a physically sensible prescription for the construction of antenna showers. These splitting functions can be used with the formulae (45), (53), (65) to generate antenna splittings in all three relevant kinematic regions. We hope that this formalism will provide a firm foundation for the construction of new parton showers based on the antenna concept.

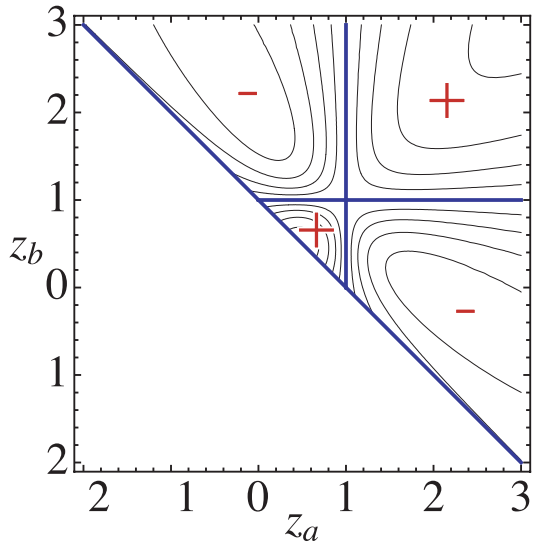

Figure 10: Visualization of the ratio of the Gehrmann-De Ridder antenna function to our antenna function for the process $g_- g_+ \to ggg$. The antenna function for the process $g_+ g_+ \to ggg$ coincides with the Gehrmann-De Ridder result and so is not included. The notation is as in Fig. 7.

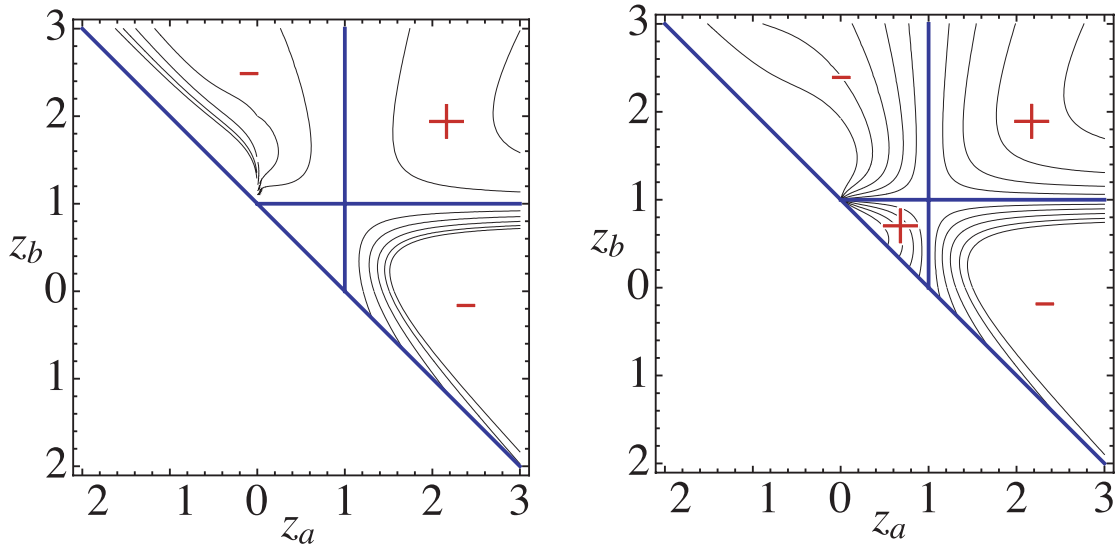

Figure 11: Visualization of the ratio of the Gehrmann-De Ridder antenna functions to our antenna functions for the processes $qg \to qgg$. The figures on the left and right are the comparison of the Gehrmann-De Ridder antenna function to our spin-summed antenna functions from row 7 and row 8 in Table 1, respectively. The notation is as in Fig. 7.

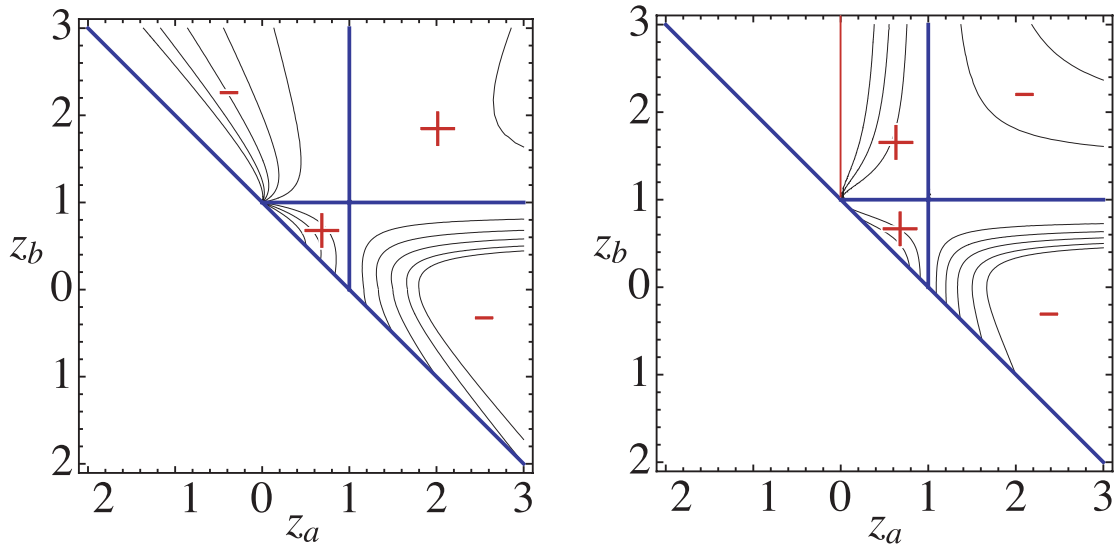

Figure 12: Visualization of the ratio of the Gehrmann-De Ridder antenna functions to our antenna functions for the processes $qg \to qq\bar{q}$. The figures on the left and right are the comparison of the Gehrmann-De Ridder antenna function to our spin-summed antenna functions from row 9 and row 10 in Table 1, respectively. The notation is as in Fig. 7.

ACKNOWLEDGEMENTS

We thank Darren Forde, Tanju Gleisberg, Peter Skands, and Jan Winter for instructive discussions and Claude Duhr and Fabio Maltoni for a useful correspondence. This work was aided by our participation in the Northwest Terascale Workshop on Parton Showers and Event Structure at the LHC at the University of Oregon. We thank the participants and, especially, the organizer, Davison Soper. The work was supported by the US Department of Energy under contract DE–AC02–76SF00515.

References

[1] T. Sjostrand, S. Mrenna and P. Skands, JHEP **0605**, 026 (2006) [arXiv:hep-ph/0603175].

[2] G. Corcella *et al.*, JHEP **0101**, 010 (2001) [arXiv:hep-ph/0011363], arXiv:hep-ph/0210213.

[3] G. Altarelli and G. Parisi, Nucl. Phys. B **126**, 298 (1977).

[4] Y. L. Dokshitzer, Sov. Phys. JETP **46**, 641 (1977) [Zh. Eksp. Teor. Fiz. **73**, 1216 (1977)].

[5] G. Marchesini and B. R. Webber, Nucl. Phys. B **238**, 1 (1984).

[6] G. Gustafson and U. Pettersson, Nucl. Phys. B **306**, 746 (1988); B. Andersson, G. Gustafson and L. Lonnblad, Nucl. Phys. B **339**, 393 (1990).

[7] U. Pettersson, Lund preprint LU-TP-88-5 (1988); L. Lonnblad, Comput. Phys. Commun. **71**, 15 (1992).

[8] W. T. Giele, D. A. Kosower and P. Z. Skands, Phys. Rev. D **78**, 014026 (2008) [arXiv:0707.3652 [hep-ph]].

[9] J. C. Winter and F. Krauss, JHEP **0807**, 040 (2008) [arXiv:0712.3913 [hep-ph]].

[10] M. E. Peskin, in preparation.

[11] S. Catani and M. H. Seymour, Phys. Lett. B **378**, 287 (1996), [arXiv:hep-ph/9602277]. Nucl. Phys. B **485**, 291 (1997) [Erratum-ibid. B **510**, 503 (1998)] [arXiv:hep-ph/9605323].

[12] D. A. Kosower, Phys. Rev. D **57**, 5410 (1998) [arXiv:hep-ph/9710213].

[13] J. M. Campbell and E. W. N. Glover, Nucl. Phys. B **527**, 264 (1998) [arXiv:hep-ph/9710255].

[14] S. Catani and M. Grazzini, Phys. Lett. B **446**, 143 (1999) [arXiv:hep-ph/9810389].

[15] C. Duhr and F. Maltoni, JHEP **0811**, 002 (2008) [arXiv:0808.3319 [hep-ph]].

[16] A. Gehrmann-De Ridder, T. Gehrmann and E. W. N. Glover, Phys. Lett. B **612**, 49 (2005) [arXiv:hep-ph/0502110], Phys. Lett. B **612**, 36 (2005) [arXiv:hep-ph/0501291], JHEP **0509**, 056 (2005) [arXiv:hep-ph/0505111].

[17] In writing a parton shower for $e^+e^- \to q\overline{q}$, one might pick up an obvious $1/N_c$ correction by writing the prefactor as $\frac{8}{3}$ instead of 3 for the first gluon emission from the quark line. In higher orders, the analogous treatment of radiation from quark lines is not so innocent and can potentially lead to incorrect accounting of color coherence.

[18] M. L. Mangano and S. J. Parke, Phys. Rept. **200**, 301 (1991) [arXiv:hep-th/0509223].

[19] L. J. Dixon, in *QCD and Beyond: TASI 1995*, D. E. Soper, ed. (World Scientific, 1996) arXiv:hep-ph/9601359.

[20] L. J. Dixon, E. W. N. Glover and V. V. Khoze, JHEP **0412**, 015 (2004) [arXiv:hep-th/0411092].

[21] R. Kleiss and W. J. Stirling, Nucl. Phys. B **262**, 235 (1985).

[22] M. P. Le and M. E. Peskin, in preparation.

[23] A. Daleo, T. Gehrmann and D. Maitre, JHEP **0704**, 016 (2007) [arXiv:hep-ph/0612257].

[24] Compare eq. (5.15) of [23].

[25] The problematical terms appear to have been simply omitted in the parton shower model of [9]. We thank Jan Winter for an extensive discussion of this point.

[26] This expression actually differs from the one given in [16] by a factor of 1/3, which comes from allowing any gluon to become collinear with any other gluon. Since we have identified the radiated gluon, we remove this factor.